



### Key Points:

- Satellite gravimetry (GRACE) was used to correct for instrumental drift in bottom pressure recorders
- Transbasin external transports at 26°N from the RAPID array were validated using 10 years of bottom pressure data
- Variability in the external transport is concentrated west of the Mid-Atlantic Ridge

### Correspondence to:

E. L. Worthington,  
emma.worthington@soton.ac.uk

### Citation:

Worthington, E. L.,  
Frajka-Williams, E., &  
McCarthy, G. D. (2019). Estimating  
the deep overturning transport variabil-  
ity at 26°N using bottom pressure  
recorders. *Journal of Geophysical  
Research: Oceans*, 124, 335–348.  
<https://doi.org/10.1029/2018JC014221>

Received 28 MAY 2018

Accepted 19 DEC 2018

Accepted article online 21 DEC 2018

Published online 15 JAN 2019

## Estimating the Deep Overturning Transport Variability at 26°N Using Bottom Pressure Recorders

**E. L. Worthington<sup>1</sup> , E. Frajka-Williams<sup>1</sup> , and G. D. McCarthy<sup>2,3</sup>**

<sup>1</sup>Ocean and Earth Science, University of Southampton, Southampton, UK, <sup>2</sup>National Oceanography Centre, Southampton, UK, <sup>3</sup>Now at ICARUS, Department of Geography, Maynooth University, Maynooth, UK

**Abstract** The RAPID mooring array at 26°N in the Atlantic has been observing the Atlantic meridional overturning circulation (AMOC) since 2004, with estimates of AMOC strength suggesting that it has declined over the 2004–2016 period. When AMOC transport is estimated, an external transport is added to the observed Ekman, Florida Straits, and baroclinic geostrophic transports to ensure zero net mass transport across the section. This approach was validated using the first year of RAPID data by estimating the external component directly from in situ bottom pressure data. Since bottom pressure recorders commonly show low-frequency instrument drift, bottom pressure data had to be dedrifted prior to calculating the external component. Here we calculate the external component from 10 years of in situ bottom pressure data and evaluate two choices for dedrifting the records: traditional and adjusted using a Gravity Recovery and Climate Experiment (GRACE) bottom pressure solution. We show that external transport estimated from GRACE-adjusted, in situ bottom pressure data correlates better with the RAPID compensation transport ( $r = 0.65, p < 0.05$ ) than using individually dedrifted bottom pressure recorders, particularly at low frequencies on timescales shorter than 10 years, demonstrating that the low-frequency variability added from GRACE is consistent with the transport variability at RAPID. We further use the bottom pressure-derived external transport to evaluate the zonal distribution of the barotropic transport variability and find that the transport variability is concentrated west of the Mid-Atlantic Ridge rather than uniformly distributed across the basin, as assumed in the RAPID calculation.

**Plain Language Summary** Differences in bottom pressure between locations in the ocean can tell us how water moves between them. We can measure it using recorders at the seabed, but because of the great depth and pressure, the measurements record a “drift” as well as changes in pressure. Removing this drift can also remove genuine longer-term signals. We try to use a completely separate measure of ocean bottom pressure, derived from satellite data, to remove this drift but keep all the real changes in pressure. To see how well this works, we compare the large-scale ocean transport we estimate using our satellite-adjusted bottom pressures, to estimates of the same transport in the North Atlantic measured by a permanent mooring array between 2004 and 2014.

### 1. Introduction

The Atlantic meridional overturning circulation (AMOC) is a key component of the climate system, comprising northward transport of warm upper waters and southward transport of deep cold water. The AMOC carries almost 90% of the approximately 1.3 PW of heat carried poleward by the North Atlantic, and AMOC strength and heat transport are strongly correlated for the seasonal timescale and at 26°N (Johns et al., 2011). Since most of the heat carried by the upper limb of the AMOC is lost to the atmosphere as it moves poleward, it plays a vital role in maintaining the milder climate of northwest Europe (Rhines et al., 2008). The Intergovernmental Panel on Climate Change state that it is unlikely that the AMOC will shut down entirely during this century but that a slowdown due to increasing anthropogenic greenhouse gas emissions is likely to occur by 2050 (medium confidence), based on coupled climate model simulations (Stocker et al., 2013). Global climate models simulating an AMOC shutdown show widespread cooling in northwest Europe and the North Atlantic, relative to rising global temperatures, together with changes to precipitation patterns and more winter storms (Jackson et al., 2015). Based on its role in the Earth’s energy budget and the potential for it to slow down, the AMOC has been measured at 26°N in the Atlantic since 2004 by the RAPID Climate Change measurement program, a joint UK/U.S. effort, which we will refer to as RAPID.

©2018. The Authors.

This is an open access article under the terms of the Creative Commons Attribution License, which permits use, distribution and reproduction in any medium, provided the original work is properly cited.

Estimates produced by RAPID suggest that the AMOC is in a reduced state (Smeed et al., 2018), with less northward transport of warm water near the surface and less southward transport at depth. The deep return flow showed a reduction of 7% per year between 2004 and 2012 (Smeed et al., 2014).

Bottom pressure recorders (BPRs) making a time series of ocean pressure at a single location are deployed as part of the RAPID array; however, bottom pressure (BP) is not used in the RAPID AMOC. A critical limitation of BPRs is that they are subject to instrumental drift, which introduces errors on timescales exceeding half the deployment period. Watts and Kontoyiannis (1990) found that instrument drift could be equivalent to as much as several centimeters of water height, compared to typical BP subannual variability equivalent to 1-cm liquid water (Kanzow et al., 2005) and that the drift varied in magnitude and sign even between the same recorder type. The drift is typically removed using an exponential-linear fit whose parameters are determined from a least squares fit to the data; however, the removal does not distinguish between instrument drift and any true low-frequency signal (i.e., with a period longer than half the record length). As a consequence, BP records can typically measure only relatively high frequency signals (annual and shorter, for a 2-year deployment period).

GRACE (Gravity Recovery and Climate Experiment) is a joint U.S./German satellite mission that was launched on 17 March 2002 and operated until it was decommissioned in October 2017. Its twin satellites orbited 220 km apart at an altitude of around 400 km and detected changes in gravity, which, over the ocean, are associated with variations in water column mass. The GRACE postprocessing center at the Jet Propulsion Laboratory (JPL) produces a global, monthly grid of ocean bottom pressure within 3° “mascons,” or mass concentration blocks. Leakage of terrestrial signals into an oceanic mascon can occur due to a single mascon overlying both land and ocean areas or due to large-amplitude terrestrial signals influencing the derived bottom pressure values in an oceanic mascon. A Coastal Resolution Improvement (CRI) filter applied to the mascon solution improves leakage errors (Watkins et al., 2015). Noise levels can also be high, although the latest data set has an improved signal-to-noise ratio relative to previous releases (Chambers & Bonin, 2012). Other GRACE products (mascon and nonmascon) are provided by Center for Space Research (University of Texas) and GFZ (GeoForschungsZentrum, Potsdam) data centers.

Several studies have compared GRACE bottom pressure measurements with ocean models (Bingham & Hughes, 2006) and observations. Fundamentally, an in situ BPR will measure the local signals at a point in the ocean, while the GRACE solution is large scale (roughly 3°). In areas where there is high variability on sub-3° spatial scales, agreement between in situ sensors and GRACE is likely to be reduced. A study by Park et al. (2008) compared GRACE Release-04 (RL04) bottom pressure data with measurements from the Kuroshio Extension System Study, an array of 46 BPRs over a 600-km<sup>2</sup> area off the east coast of Japan. The spatially averaged, monthly mean BPR data showed strong correlation with the GRACE bottom pressure data. The correlation between individual recorder and GRACE bottom pressures was reduced by small-scale variability, with low (high) correlation for sites with high (low) eddy kinetic energy. Macrander et al. (2010), who compared BP data from 100 locations around the world with several (nonmascon) GRACE solutions, found that correlation was generally good at high latitudes and poor at low latitudes. At midlatitudes, correlation was more dependent on the GRACE product used. Kuroshio Extension System Study BP agreed well with JPL and Center for Space Research products (Park et al., 2008), whereas RAPID BP correlated best with GFZ products (Macrander et al., 2010). Böning et al. (2008) found that in situ BP anomalies and GRACE values showed better agreement when the in situ BP records were spatially coherent, indicating that the dominant signal in the individual records was associated with a large-scale BP anomaly. They further found that the spatial coherence in in situ BP records was linked to bottom topography. Landerer et al. (2015) used GRACE BP anomalies from JPL Release-05 (RL05) to estimate the deep ocean transports, finding that GRACE-derived estimates of transport recovered the magnitude and variability ( $r = 0.69$ , after detrending and low-pass filtering) of the Lower North Atlantic Deep Water transports (3,000–5,000 m) at 26°N. The Lower North Atlantic Deep Water transport is part of the southward return flow of the AMOC and correlates strongly with the total AMOC variability at 26°N. The studies briefly described above show that GRACE can be useful in observing ocean circulation changes.

AMOC transport at 26°N is estimated using the approach described in McCarthy et al. (2015), where three main components are determined from measurements and the fourth is a residual. The Gulf Stream transport (TGS) within the Florida Straits is measured by submarine cables and calibrated by regular hydrographic sections (Meinen et al., 2010; Baringer & Larsen, 2001). The Ekman transport component (TEK) is

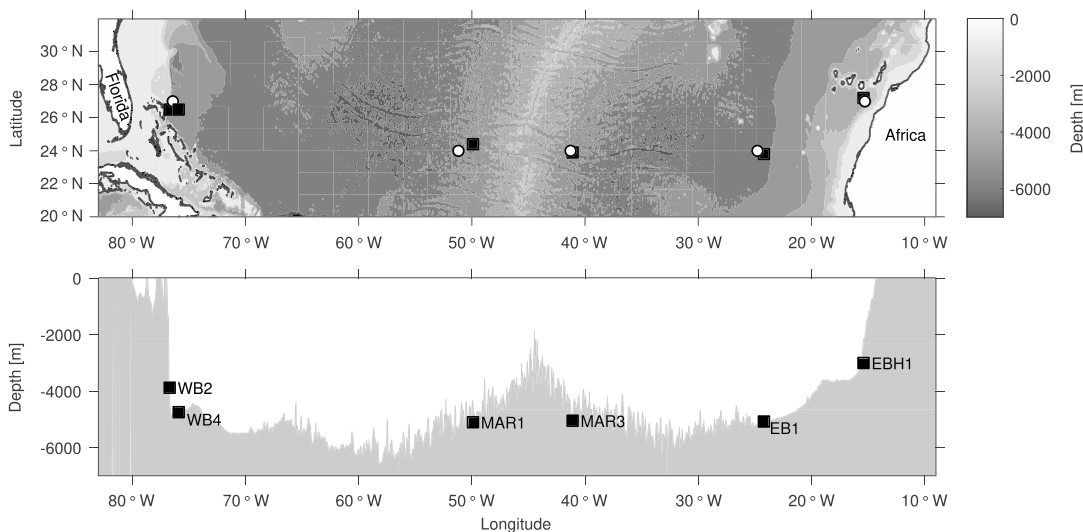


**Figure 1.** The distribution of RAPID moorings along 26.5°N in the subtropical North Atlantic as a plan view (top) and section (bottom). Black squares show the location of bottom pressure recorders, and white circles show the center position of the closest GRACE mascon (Bathymetry data from the GEBCO\_2014 Grid, version 20150318, [www.gebco.net](http://www.gebco.net)).

calculated from ERA-Interim reanalysis wind fields. The internal transport (*TINT*) between the Bahamas at 77°W and the Canary Islands at 14°W is determined from two different sources: (1) direct current meter measurements between the Bahamas at 77°W and 76.75°W, a component referred to as the Western Boundary Wedge, and (2) mid-ocean geostrophic flow is estimated from dynamic height moorings between 76.75°W and the Canary Islands relative to a deep reference level (4,820 dbar). The moorings at the western and eastern boundaries are merged to obtain the dynamic height profiles, which are used to calculate eastern and western basin transports. Antarctic Bottom Water transport is included as a time-invariant profile below the reference level. The external transport (*TEXT*), referred to hereafter as the hypsometric compensation to distinguish it from the BP-derived external transport, is an additional transport that when added to the other components gives a zero net flow at each depth across the section:

$$T(z, t) = T_{GS}(z, t) + T_{EK}(z, t) + T_{INT}(z, t) + T_{EXT}(z, t), \quad (1)$$

where

$$\int_{z_{\text{bottom}}}^0 T(z, t) dz = 0. \quad (2)$$

The justification for this approach is that the volume of the North Atlantic north of 26°N is conserved between 5 and 10 days (Bryden et al., 2009), as the small inputs and outputs ( $\mathcal{O}(1 \text{ Sv})$ ) are balanced. This method was initially validated for periods longer than 15 days in a study by Kanzow et al. (2007, hereafter referred to as K07). They found a strong correlation ( $r = 0.82$ ) between AMOC transports estimated using the components described above (TGS, TEK, and TINT) added to (1) hypsometric compensation assuming zero net flow across the section and (2) an external transport calculated from in situ bottom pressure data from a single year. The hypsometric compensation method has been used since 2004 by the RAPID project in estimating AMOC transports. In this paper, we do not attempt to validate this assumption. Instead, we use the RAPID estimate of the hypsometric compensation to validate a bottom pressure approach to estimating the external transports at 26°N with two different drift correction methods.

In section 2, we give an overview of the data sets used and processing applied. In section 3, we describe the two drift correction methods used (with and without GRACE). Section 4 reports the results including using the bottom pressure-derived external transports to investigate the zonal distribution of transport variability and long-term variations. We conclude in section 5.

## 2. Data

### 2.1. Bottom Pressure

The BPRs used by the RAPID project are accurate to better than 0.01 dbar (Meinen et al., 2013). The mooring deployments varied in length: Early moorings were deployed for 1 year, but most were routinely deployed as

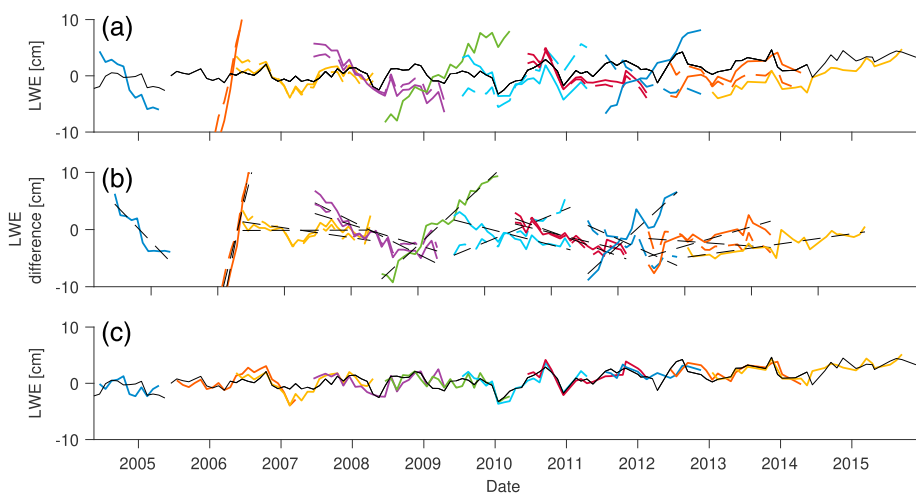


**Figure 2.** Using GRACE data to adjust WB2 mooring BPR data for instrument drift. (a) Comparison of BP (as LWE) from individual deployment BPR (colored lines) and GRACE (black line). Where two BP recorders were deployed together, solid and dashed lines are shown in the same color. (b) The difference between recorder and GRACE bottom pressures (colored lines) with a linear fit to each (dashed black line). (c) Comparison of GRACE-adjusted (instrument drift removed) BPR (colored lines) and GRACE BP (black line). Where two recorders were deployed, the mean postadjusted value was used. Equivalent figures for WB4, EB1, and EBH1 are available in the supporting information (Figures S2–S4). LWE = liquid water equivalent; GRACE = Gravity Recovery and Climate Experiment; BPR = bottom pressure recorder; BP = bottom pressure.

pairs of recorders for 2 years, overlapping with the following recorder pair by 1 year. Here we focus on four sites: two from the eastern boundary (EB1 and EBH1) and two from the western boundary (WB2 and WB4), covering the period from 18 May 2004 to 23 May 2014 (the start and end dates common to all moorings). The mooring positions of the RAPID array are shown in Figure 1. Some records are missing due to instrument loss or failure. One record from each of WB2 and EB1 was discarded due to obvious instrument error; however, there were concurrent data available. Two moorings already had significant data gaps due to instrument failure or loss: EB1 had a gap of 139 days between 7 March 2006 and 24 July 2006 and EBH1 had a gap of 153 days between 5 December 2005 and 5 July 2006. Data from two Mid-Atlantic Ridge (MAR) moorings, MAR1 and MAR3, were also available. Including these moorings makes little difference to external transport variability (see also supporting information, K07), so they are not included when calculating TEXT; however, they were included when comparing the zonal distribution of the external transport variability. The amplitude of bottom pressure signals associated with the tides is approximately an order of magnitude greater than those associated with the external transport. To remove the tides, bottom pressure records (BPR) from RAPID mooring deployments (Smeed et al., 2015) were detided using harmonic fits to tidal constituents (Intergovernmental Oceanographic Commission, 2002), then filtered using a 1.625-day Tukey filter, which was a modification of the recommended method used for its improved spectral properties.

The GRACE data set used was version 2 of the JPL GRACE Mascon Equivalent Water Height RL05M.1 (Watkins et al., 2015; Wiese et al., 2016, 2015), which reports ocean bottom pressure as liquid water equivalent (LWE) in centimeters within mascons, which are equal-area  $3^{\circ}$  spherical-cap cells. JPL employs a CRI filter that reduces leakage errors when a mascon covers both land and ocean. GRACE data sets are available at <http://grace.jpl.nasa.gov>, supported by the National Aeronautics and Space Administration MEASUREs (Making Earth System Data Records for Use in Research Environments) Program. The JPL RL04 data set was shown to correlate well with in situ bottom pressure measurements by Park et al. (2008; see section 1), and the RL05 data set has an improved signal-to-noise ratio compared to RL04 (Chambers & Bonin, 2012). Ocean bottom pressure time series derived from mascon solutions show improved correlation with in situ data than those derived from the alternative spherical harmonic

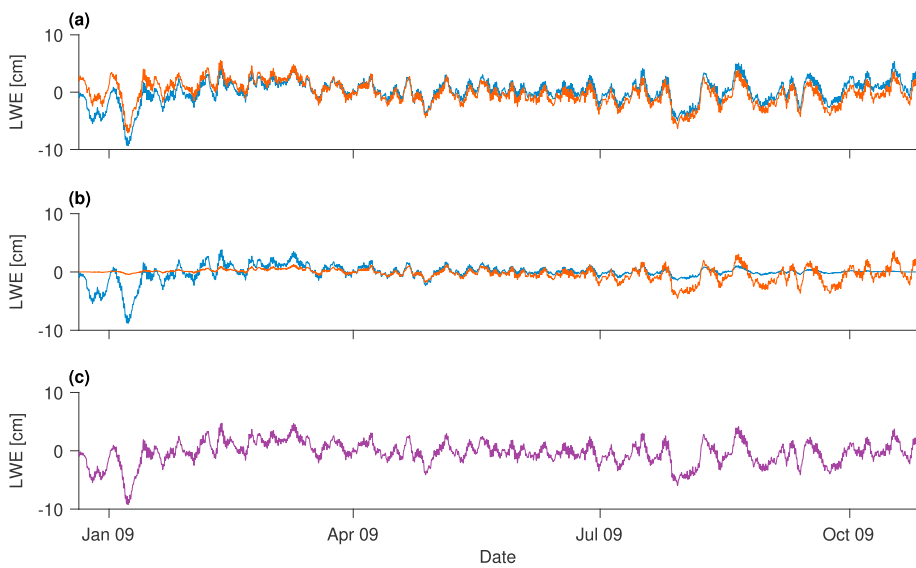


**Figure 3.** Replacement of overlapping sections by mean of weighed overlaps. (a) Unweighted overlapping sections of two EB1 mooring bottom pressure records, from deployments EB1L7 (blue) and EB1L8 (red). EB1L7 was deployed from 6 January 2011 to 23 October 2012, and EB1L8 from 25 September 2011 to 24 May 2014. After removal of the first 50 days, they overlapped by 348 days between 10 November 2011 and 23 October 2012 as shown. (b) Overlapping sections of the two EB1 mooring deployments, EB1L7 (blue) has been multiplied by a weighting that decreases linearly from 1 to 0, and EB1L8 (red) by one that increases linearly from 0 to 1. (c) Mean of weighted overlapping sections. LWE = liquid water equivalent.

solutions, especially at lower latitudes where the signal-to-noise ratio is lower (Watkins et al., 2015). The RL05M.1 data set provides a LWE thickness in centimeters gridded to a regular  $0.5^{\circ}$  grid of latitude and longitude. The time resolution is not fixed but is approximately 30 days. Corrections for viscoelastic glacial isostatic adjustment trends had already been made to the data following the model by Geruo et al. (2013).

Additional data used from the RAPID program were in situ temperature and practical salinity time series given at 20-dbar pressure intervals for individual deployments for the moorings EB1 ( $26.8^{\circ}\text{N}$ ,  $24.2^{\circ}\text{W}$ ) and WB4 ( $26.5^{\circ}\text{N}$ ,  $75.7^{\circ}\text{W}$ ). There were small data gaps of a few days between each deployment and a couple of larger gaps (approximately 1 year in length) where moorings were lost. Data gaps longer than a few days were filled using the depth-mean temperature and salinity for the whole mooring; short gaps between deployments were filled by linear interpolation. The RAPID project also provided hypsometric compensation data determined relative to 4,820 dbar from 2 April 2004 to 11 October 2015 and given every 20 dbar. RAPID project data had already been detided with a 2-day fifth-order Butterworth filter. Hydrographic data for  $26^{\circ}\text{N}$  from 2010 provided in situ temperature and practical salinity measurements along the RAPID mooring latitude.

### 3. Methods

#### 3.1. Drift Removal in Bottom Pressure Records

Instrument drift is typically exponential at the beginning of a bottom pressure record, combined with a linear drift throughout (Johns et al., 2005) and is normally dealt with by removing a simple least squares exponential-linear fit (Cunningham, 2009; Watts & Kontoyiannis, 1990). However, using this method, some of the linear decay may project onto an exponential decay timescale, resulting in computed decay timescales of up to 671 days. More recently, enabled by the 1-year overlaps between bottom pressure deployments, an exponential-linear drift was fit to the 1-year overlap period between two overlapping 2-year records. Using this approach, the exponential decay scale was typically no longer than 100 days, with a mean (median) decay scale of 42 (43 days). Due to uncertainties in the drift calculation from BPR records, and because drift characteristics from individual sensors do not always follow an exponential-linear decay, we have instead chosen to remove the first 50 days of each record, since most of the nonlinear behavior in individual records occurs during this time period (Figure S1 in the supporting information). The overlapping deployments allowed continuous time series to be obtained at most locations (Figure 2a), with the exception of a 50-day

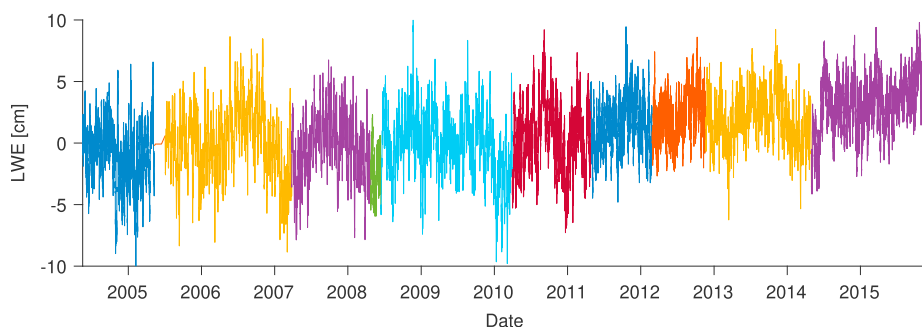


**Figure 4.** Complete bottom pressure (as liquid water equivalent, or LWE) time series for the WB2 mooring; adjusted for instrument drift using Gravity Recovery and Climate Experiment data, with data gaps filled with a modified annual cycle, and with overlapping sections replaced by a weighted mean.

gap at the WB4 mooring from 27 April 2009. The lengths of gaps at EB1 and EBH1 described in section 2.1 were also increased by 50 days. The hydrostatic balance  $P = \rho gh$  was used to convert between BP and LWE (GRACE BP), with the average density  $\rho$  estimated for the mooring from hydrographic data, and local gravity  $g$  from the mooring latitude and depth  $h$ . Individual BP records were then binned in time to match the time resolution of the GRACE time series. The GRACE BP for that time period and nearest mascon was subtracted from the binned BP records and a line fit to the difference (Figure 2b). This linear fit was then removed from the BP record to remove the drift in the BP record not associated with variability in the GRACE data (Figure 2c). Where two simultaneous records were available, they were averaged.

To create full time resolution records at each mooring location, the same linear fits were applied to individual BP records (after removing the first 50 days). Data gaps in the GRACE-adjusted time series were longer than 50 days, so were filled using a technique following DiNezio et al. (2009). For overlapping sections at full time resolution, records were interpolated onto a time grid associated with the higher sampling frequency (Figure 3a). Overlapping sections were weighted, with the weighting decreasing linearly from 1 to 0 for the ending section and increasing linearly from 0 to 1 for the starting section (Figure 3b). The mean of the weighted sections (Figure 3c) was used to replace the overlap.

### 3.2. Estimation of External Transport Variability

Vertically integrated external transport variability (TEXT) can be estimated as the sum of the transport variability between mooring pairs, as

$$T_{\text{ext}} = \frac{H_{\text{ebh1}}}{f\rho} [P_{\text{ebh1}} - P_{\text{eb1}}] + \frac{H_{\text{wb4}}}{f\rho} [P_{\text{ebh1}} - P_{\text{wb4}}] + \frac{H_{\text{wb2}}}{f\rho} [P_{\text{wb4}} - P_{\text{wb2}}] \quad (3)$$

where  $P$  is the fluctuation in bottom pressure at a given mooring,  $f$  is the Coriolis parameter,  $\rho$  is density, and  $H$  is the water column height at the shallower mooring of the pair (K07). Transport variability is calculated from the complete time series of GRACE-adjusted BP records (Figure 4).

Since moorings are at different depths, hydrostatic pressure due to density fluctuations between the two depths was used to adjust the pressure at the deeper mooring level to the shallower. For each deeper mooring of a pair, the in situ temperature and practical salinity were converted to conservative temperature and absolute salinity, which were then used to obtain the steric height relative to the deeper mooring pressure

**Table 1**

*Mooring Depth Ranges and Median Values, and the Reference Pressure Used for Each to Determine the Steric Height, if Applicable (Only Applies to the Deeper of a Mooring Pair)*

Mooring	Nearest GRACE mascon ID	Minimum depth (m)	Maximum depth (m)	Median depth (m)	Reference pressure (dbar)
WB2	1,271	3,863	3,898	3,884	N/A
WB4	1,271	4,691	4,821	4,745	4,580
EB1	1,395	5,000	5,104	5,092	4,960
EBH1	1,289	2,993	3,024	3,007	N/A

*Note.* N/A = not available; GRACE = Gravity Recovery and Climate Experiment.

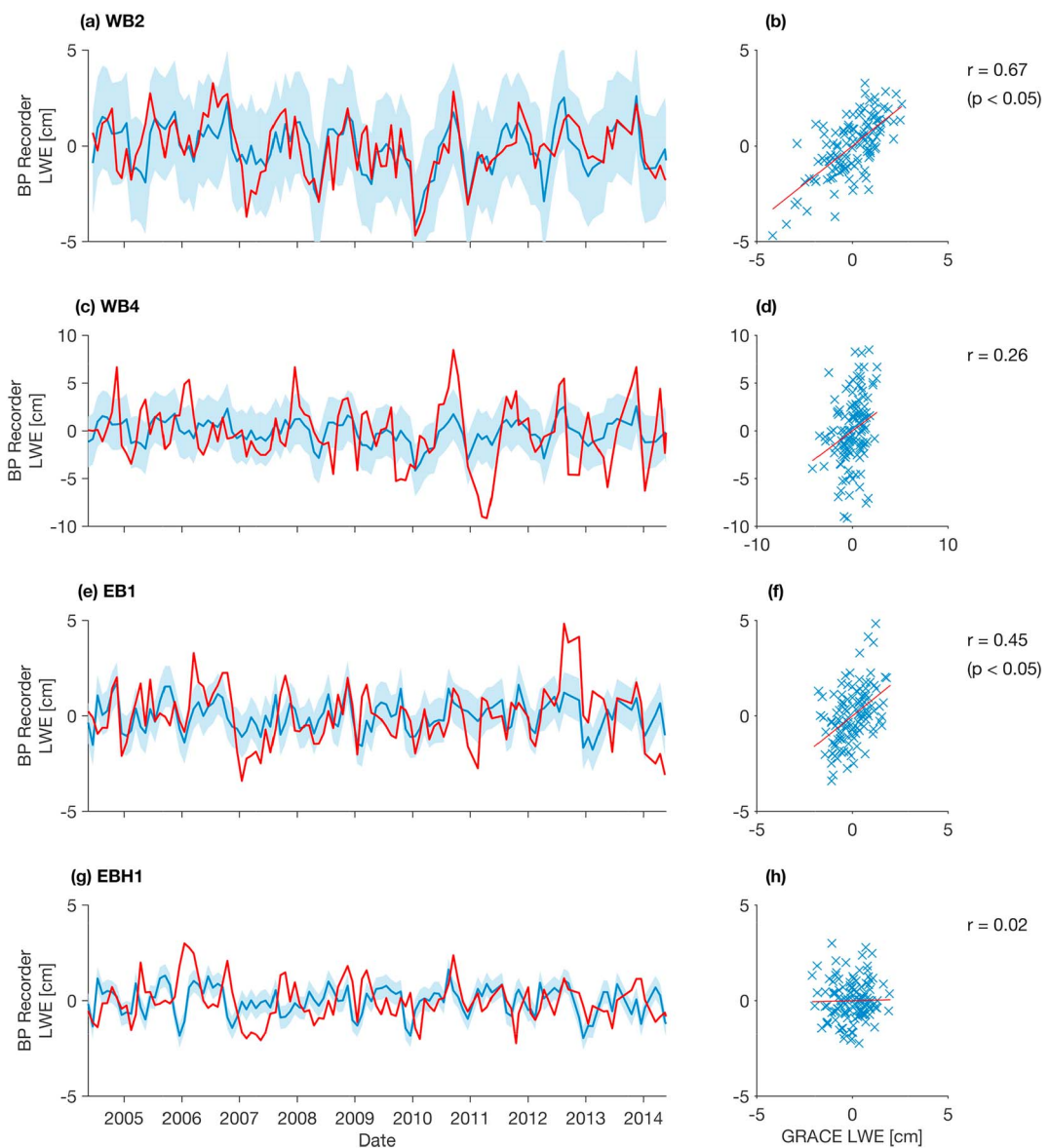


**Figure 5.** (a, c, e, and g) Comparison of monthly averaged BP (LWE) from recorders (red) and GRACE (blue), with the uncertainty of GRACE LWE (cm) shown by the light blue shading. (b, d, f, and h) Scatter plots for the same data showing correlation coefficient  $r$  and significance (if significant), with the red line indicating the best linear fit. Data shown for moorings WB2 (a, b), WB4 (c, d), EB1 (e, f), and EBH1 (g, h). GRACE = Gravity Recovery and Climate Experiment; LWE = liquid water equivalent; BP = bottom pressure.

(McDougall & Barker, 2011). Ideally, the pressure at the deeper mooring would be used as a reference; however, the temperature and salinity data at moorings WB4 and EB1 did not reach the full depth, so the deepest pressure common to all records for a mooring was used instead. Details of the mooring depths and reference pressures used are given in Table 1. Once the steric height was determined relative to the reference pressure, the time mean was subtracted to give the steric height variability. This was then added to the deeper mooring LWE thickness, to remove the pressure contribution due to density fluctuations between the shallower and deeper mooring depths. The shallower mooring depth was used as  $H$  in equation (3).

The difference in hydrostatically adjusting BP between moorings was used to estimate the external transport for mooring pairs WB2-WB4, WB4-EB1, and EB1-EBH1. The external transport at 26°N was then estimated as the sum of these three components (equation (3)). Finally, all component and total transport estimates and the hypsometric compensation were smoothed using a 15-day Tukey window to remove high-frequency

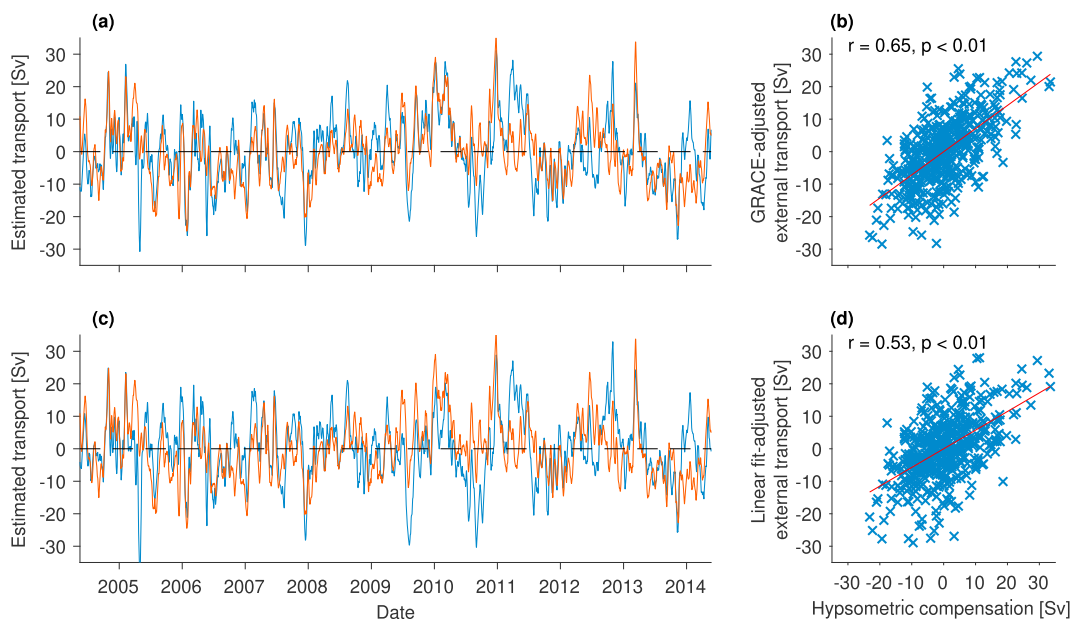


**Figure 6.** Time series for hypsometric compensation (red) and BP-determined external transport (*TEXT*; blue), with a dashed line marking zero anomaly. The figure shows the comparison of both methods to adjust BP for recorder drift, (a) using linear fit to difference between recorder and GRACE data and (c) using linear fit to the recorder data itself. (b) and (d) Scatter plots for the same data, with the red line showing the best linear fit. BP = bottom pressure; GRACE = Gravity Recovery and Climate Experiment.

variability, since K07 showed that the compensation was appropriate on timescales longer than 10 days. These smoothed time series are used for the comparisons in section 4.

In order to evaluate the efficacy of using GRACE data to adjust the mooring data from instrument drift, individual bottom pressure records were also corrected using a simple linear fit to the in situ BP record. The in situ BP data were again averaged over the same time intervals as the GRACE data (after removing the first 50 days of each record) and a linear fit made to each deployment. This was subtracted from the full time resolution bottom pressure records (first 50 days removed) and a transport time series for each mooring obtained using the same methods described above. All linear regressions were determined using a least squares fit and Pearson's correlation coefficient, with confidence intervals determined according to Bendat and Piersol (2010). For degrees of freedom of the time series, these were calculated from the integral timescale of decorrelation (Thomson & Emery, 2014). All correlation coefficients are significant at the 95% level unless otherwise stated. Coherence was calculated using a multitaper spectrum following Percival and Walden (1998), which reduces spectral leakage while minimizing the data loss associated with other tapers.

## 4. Results

### 4.1. External Transports Compared to RAPID Compensation Term

BP variability derived from the recorder data at WB2 shows a strong correlation with the GRACE ocean BP data for the closest mascon ( $r = 0.67$ , Figure 5b) and is well within the uncertainty (Figure 5a), whereas the BP variability at EBH1 shows almost no correlation with the corresponding GRACE data ( $r = 0.02$  and not significant, Figure 5h) and frequently exceeds the GRACE BP uncertainty (Figure 5g). Correlations between the other mooring BP records and the ocean BP from the nearest GRACE mascon vary from weak (WB4,  $r = 0.26$  and not significant) to moderate (EB1,  $r = 0.45$ ). It should be noted that both WB2 and WB4 BP are compared with BP from the same GRACE mascon and that the difference in correlation is likely due to mesoscale variability being suppressed by the steep continental slope at WB2 but not at WB4 (Hughes et al., 2018; Kanzow et al., 2009). Overall, we conclude that while some GRACE BP records agree with the in situ measurements, this depends on the location. This may be due to the spatial footprint of GRACE being much larger than a point mooring deployment, which is discussed further in section 5 and may be due to intense mesoscale activity away from steep topography. To maintain common processing, the GRACE adjustment

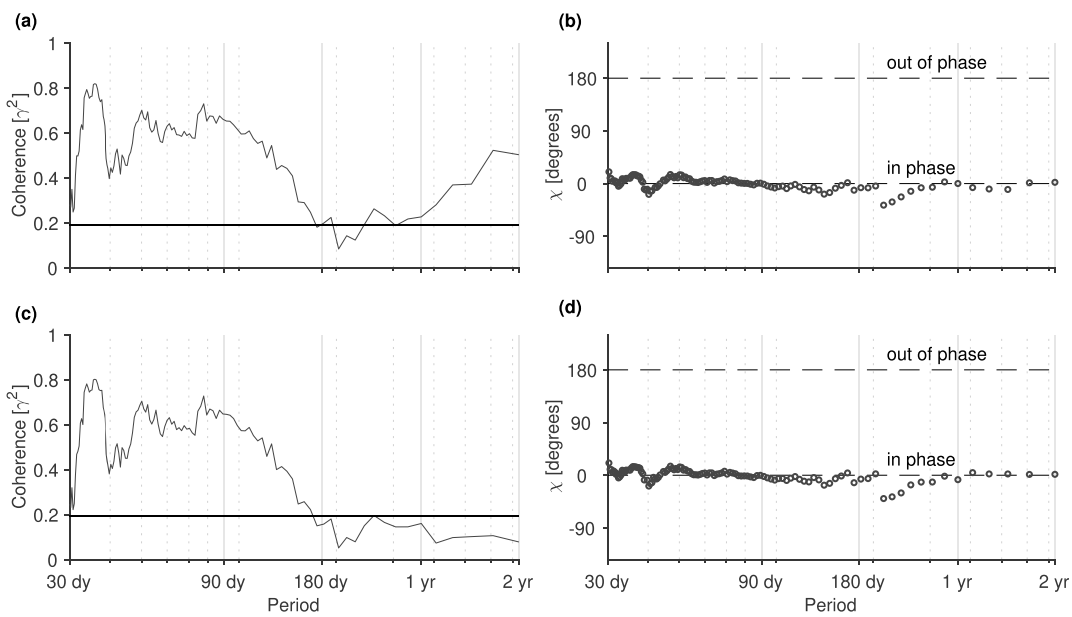


**Figure 7.** Coherence between estimated external transport and hypsometric compensation (both detrended and smoothed with a 15-day Tukey window). The figures on the left (a, c) show coherence, with significance indicated by the horizontal black line. The figures on the right (b, d) show the phase relationship for the same period. The upper figures (a, b) are for the external transport estimated using the GRACE adjustment method, and the lower (c, d) are for the “linear-fit” method.

is still used at all locations. It is possible that mesoscale variability averages to zero on longer timescales, making the GRACE record an appropriate choice for the low-frequency correction of in situ BP records.

The effectiveness of using GRACE bottom pressure data to adjust for instrument drift is examined by comparing both TEXT derived using the linear fit to the record only and TEXT derived using the linear fit to the difference between the GRACE and deployment LWE. The hypsometric compensation used here includes the MAR. The external transport correlates well to the hypsometric compensation ( $r = 0.65$ ), the residual in the RAPID AMOC transport calculation (Figure 6). They appear to correspond reasonably well over both shorter and longer timescales, with most strong peaks in hypsometric compensation (e.g., December 2007, January–March 2010, January 2011, February–April 2013, and November–December 2013) matched by a similar peak in external transport; however, there are two strong negative external transport peaks in May 2005 and 2006 where there is no corresponding hypsometric compensation peak (Figure 6a). Variability of external transport is slightly greater than that of hypsometric compensation (RMS: 10.2 vs. 9.0 Sv for the detrended, smoothed time series). The correlation between the external transport using the linear fits without GRACE and hypsometric compensation is lower ( $r = 0.52$ , Figure 6d).

The estimated GRACE-adjusted external transport and hypsometric compensation are significantly coherent and in phase for most periods between 30 and 180 days, with peaks between 30 and 40 days, around 50 days and between 75 and 100 days (Figure 7). Coherence is lower, at just above the level of significance, for periods between 180 days and 1 year. At just over 180 days, the two time series are out of phase by around 30°, equivalent to a lag of about 15 days for a period of 180 days; however, the coherence is not significant. For periods longer than a year, the coherence between external transport and hypsometric compensation increases and is in phase again. Notably, the linearly adjusted transport shows similar in-phase coherence for periods below 180 days; however, the coherence for periods greater than 180 days is much lower and not significant, demonstrating improvement on longer timescales when using the GRACE-adjusted BP records.

#### 4.2. Zonal Distribution of External Transport

Correlations between each mooring pair component and the hypsometric compensation (bottom plot) are very weak ( $r < 0.25$ ) and not significant, especially compared to the stronger correlation ( $r = 0.65$ ) between the total external transport and the hypsometric compensation. High variability at midbasin locations (e.g., WB4 or MAR1) contributes variability to both the WB2-WB4 transport pair and WB4-MAR1 transport but largely cancel when summed. To evaluate the zonal distribution of external transport, we accumulate

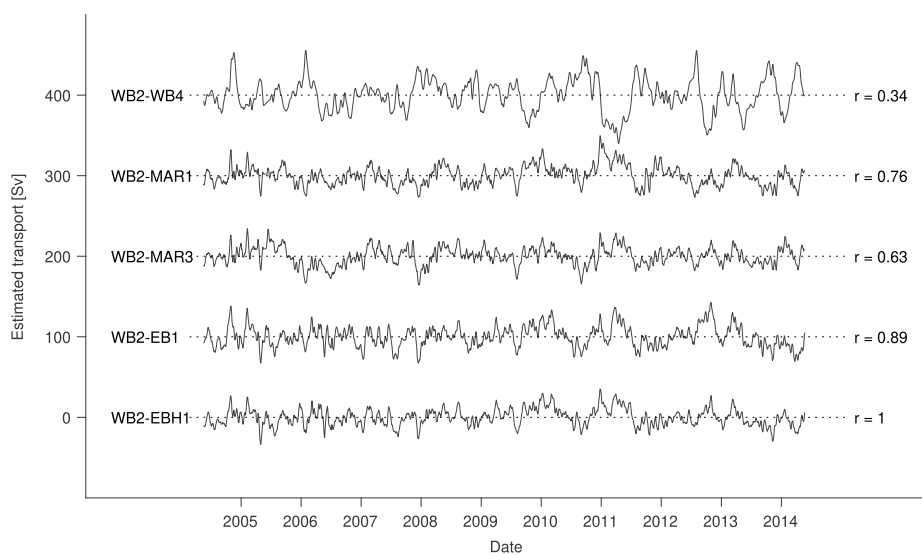


**Figure 8.** Estimated transport variability between the zonal cumulative sum of mooring pair transports compared with the total estimated transport (sum from *WB2* to *EBH1*). The correlation coefficient between each sum and the total is shown for each (each component is offset by 100 Sv for clarity and the zero transport marked with a dotted line). All time series were detrended and smoothed with a 15-day Tukey window. All *r* values are significant at the 95% level.

transports between mooring pairs from west-to-east (Figure 8). When the zonal cumulative sum of mooring pair transport variability from the westernmost to easternmost mooring is compared to the total external transport variability, the highest correlation ( $r = 0.76$ ) is seen for the zonal sum between moorings *WB2* and *MAR1* (Figure 8). For comparison, the variability captured is estimated for both a west-to-east and east-to-west accumulation, where we see that from east-to-west, significant variability is only captured when the accumulation arrives at the western boundary (Figure 9). The change in correlation between the zonal cumulative transport variability and total external transport variability with longitude shows that the external transport variability is concentrated to the west of the MAR, between the *WB2* and *MAR1* moorings ( $76.75^{\circ}\text{W}$  and  $51^{\circ}\text{W}$ ).

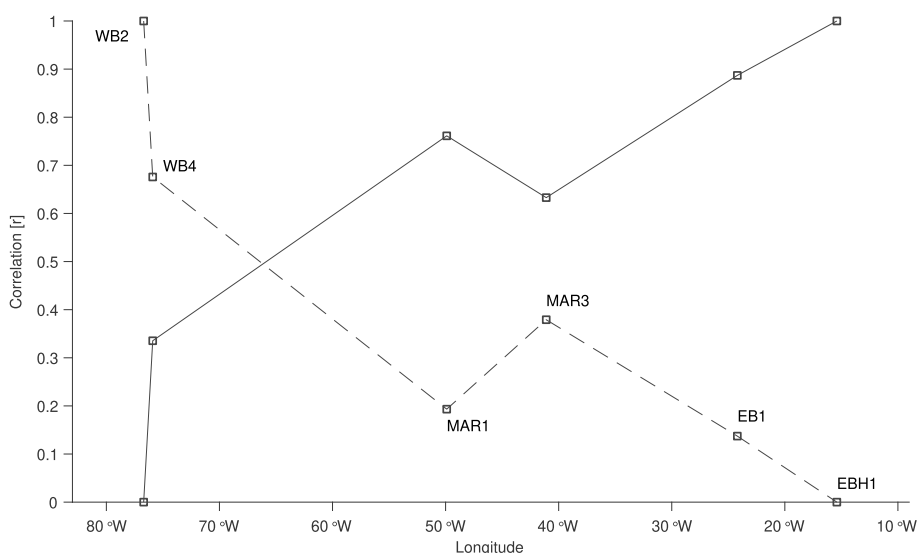


**Figure 9.** Correlation between the cumulative sum of mooring pair transport variability and the total external transport variability, plotted against longitude. The solid line shows the cumulative sum from west to east; the dotted line the sum from east to west. Squares show the mooring positions.

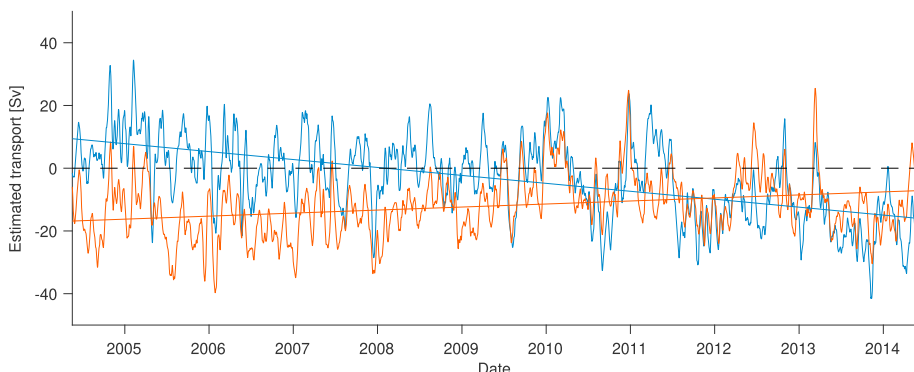


**Figure 10.** Gravity Recovery and Climate Experiment-adjusted bottom pressure-derived external transport TEXT (blue) and hypsometric compensation (red), showing the linear fit to each. Both time series are smoothed with a 15-day Tukey window but are not detrended. The dotted line marks zero transport.

#### 4.3. Trend Over 10 Years

To evaluate the longer timescale variability in the GRACE-adjusted estimate of external transport (TEXT) and hypsometric compensation, we compare the time series when both were smoothed as before but not detrended (Figure 10). A simple linear fit to both time series shows the external transport as a strengthening southward flow during the entire period, whereas the southward flow of the hypsometric compensation becomes increasingly weaker. A strengthening southward external transport is in opposition to the trend observed by the RAPID project (Smeed et al., 2014). TEXT also appears to be predominantly northward during the first two years of the record, which is physically unlikely, as it would imply a persistent net northward flow across 26°N when combined with the measured AMOC components. Over the observed 10 years, the southward hypsometric compensation weakens by around 9.5 Sv, whereas the southward external transport strengthens by over 20 Sv. Assuming the North Atlantic above 26°N has an area of approximately  $2 \times 10^{13} \text{ m}^3$ , and the other transport components remain as determined by RAPID, then a total increased southward transport of nearly 30 Sv over 10 years would result in a sea level drop northward of 26°N of over 4 m/year. Such a change has not been observed in the altimetry record. It is known that GRACE BP measurements are subject to uncertainty on longer timescales (Wahr et al., 2015) and have been detrended in other studies (Landerer et al., 2015); this is discussed further below.

### 5. Discussion and Conclusions

The GRACE-adjusted, bottom pressure-derived external transport variability and the RAPID-estimated hypsometric compensation show strong correlation ( $r = 0.65$ ) and significant in-phase coherence over timescales between 30 and 180 days and greater than one year but weaker coherence over timescales between 180 and 365 days. K07 also found that for a single year (March 2004 to March 2005), TEXT showed weak negative correlation ( $r = -0.32$ ) with TEK, which is close to the value ( $r = -0.38$ ) found for this longer time series. McCarthy et al. (2012) identified a weakening in the deep southward return flow between early 2009 and mid-2010, which is seen in the increased northward TEXT anomaly and is also a period when the agreement with the hypsometric compensation is particularly good. The strong wind event of early 2013 is also represented well by TEXT, and in general, strong peaks in hypsometric compensation coincide with strong peaks in TEXT, although the converse is not always true; strong peaks in TEXT are not always matched by strong hypsometric compensation peaks. These shorter periods of disagreement may be due to the bottom pressure records having some residual exponential drift that was not captured by the choice of removing the first 50 days. However, removing a longer period would increase the length of gaps between records. For example, the peak in external transport during early 2011 that has no corresponding hypsometric compensation peak may be due to the EB1 record for that period still having a steep decline at the beginning of the record, which neither the GRACE data nor the preceding record shows (Figure S3).

Bottom pressure variability is highest at the WB4 mooring (root-mean-square RMS: 4.1 cm) compared to WB2 and EB1 (RMS: 2.8 and 2.2 cm, respectively), and transport component variability is consequently highest (RMS: 27.9 Sv) for the main basin component (WB4-EB1). The main source of TEXT variability at the western boundary is likely to be variability of the deep western boundary current (DWBC) transport,

which is expected to be concentrated along the continental slope at 26.5°N. The variability of the DWBC transport is much greater than that of the AMOC transport (standard deviations of 16 Sv compared to 5 Sv), with baroclinic and especially barotropic flows showing variability exceeding 10 Sv on timescales of days to months (Meinen et al., 2013). The time mean eastern edge of the DWBC core (southward current speed  $>10$  m/s) is found at the approximate longitude of the WB4 mooring at around 76°W (Figure 4, Bryden et al., 2005), although it was observed to meander beyond 75.5°W during June 1990 (Figure 10, Lee et al., 1996), so it is likely that it meanders about its time mean position and across the WB4 mooring position. Meinen et al. (2013) found that bottom pressure-derived transports between mooring pairs C-D and D-E deployed at 26.5°N as part of the National Oceanographic and Atmospheric Administration Western Boundary Time Series were anticorrelated ( $r = -0.50$ ). Mooring C is between WB2 and WB4, and D and E are east of WB4, so at and beyond the edge of the time mean DWBC position. Meinen et al. (2013) attributed the anticorrelation of the mooring pair transports to meandering of the DWBC, due to the absence of lag in the correlation. It seems likely that variability of BP at WB4 is due to variability of transport and/or position of the DWBC, but without comparing it to the relevant data it is difficult to say, which, if either, is the main cause.

The generally good agreement between the GRACE-adjusted BP-derived external transport and the hypsometric compensation shows that using GRACE to adjust in situ BP records for instrument drift can be effective. However, this may be largely due to the mascon nearest the WB2 position capturing much of the transport variability. Correlation between GRACE and in situ BP can depend on bottom topography, which can affect spatial coherence and the presence of short-wavelength bottom pressure components such as mesoscale eddies (Böning et al., 2008; Macrander et al., 2010; Park et al., 2008). We found correlations between GRACE-adjusted BP records and GRACE BP data varied from  $r = 0.02$  (EBH1) to  $r = 0.67$  (WB2). WB2 and WB4 use the same GRACE mascon to provide BP data, but the equivalent correlation for WB4 is  $r = 0.26$ . Park et al. (2008) showed that if an in situ BP record is dominated by components with wavelengths shorter than the GRACE resolution of 300 km, low correlation with GRACE ocean BP can result. Near the western boundary of the North Atlantic, variability in sea surface height and eddy kinetic energy at WB4 has been found to be higher than that of moorings close to the continental slope such as WB2 (Kanzow et al., 2009). Hughes et al. (2018) showed that, in the NEMO ocean model, mesoscale variability in BP is suppressed on the continental slope. The suppression of small-scale variability by the steep western continental slope may explain the difference in correlation of in situ BP at WB2 and WB4 with the same GRACE mascon BP.

When the GRACE-adjusted external transport variability is examined without the overall trend removed, a simple linear fit suggests that the southward flow is strengthening over time. This is in opposition to the weakening southward flow of the hypsometric compensation shown here and described by Smed et al. (2014). This trend in the external transport estimate originates from low-frequency variability in the GRACE data that is introduced to the mooring bottom pressure data during the adjustment process. There are known long-period signals within GRACE data that are not completely removed during processing, for example, components of the pole tide that have interannual and decadal periods (Wahr et al., 2015). These can introduce errors in estimates of ocean mass and may be responsible for the implied strengthening of the southward flow when the 10-year trend is used in the BP dedrifting.

The error on GRACE data (see Figure 5) is large relative to the signal, introducing uncertainties in the time series at each mooring position. These, combined with the long-period signals, limit the accuracy of the correction to in situ BP records. To more rigorously assess uncertainties on the reconstructed barotropic transports, a high-resolution numerical model could be used from which GRACE-like bottom pressure and point measurements of BP could be extracted, random errors and a trend introduced to the GRACE-like data, and a drift introduced to the BP data. The dedrifting procedure outlined here could then be applied and the reconstructed transports compared to model truth. This is, however, outside the scope of the present study. In spite of issues with the long-term trends and uncertainties on the GRACE estimate of BP, GRACE's global long-term coverage has enabled the evaluation of external transport variability from BPRs at 26°N.

Overall, these results show that GRACE may be used to correct for instrumental drift in in situ bottom pressure records, enabling estimates of deep ocean transports on sub-10-year timescales but must take into account the issues presented by comparing BP measurements from a single point with GRACE BP averaged over a mascon 3° in size. At 26°N, this new estimate of external transports is fully independent of the RAPID transport estimates, and the results here demonstrate that the hypsometric compensation method

employed by RAPID is sensible and captures the external transport variability. Using the zonal distribution of in situ bottom pressure records, we show that the external transport variability is concentrated at the west but that measurements across the western basin of the Atlantic are required to capture the deep transport variability. While the external transport variability is concentrated in the west, the good agreement between the hypsometric compensation term in the RAPID method and this fully independent estimate of external transports demonstrates that on sub-10-year timescales, the hypsometric approach is justified.

## Acknowledgments

E. L. W. is funded by the Natural Environment Research Council's (NERC) SPITFIRE Doctoral Training Partnership. E. F. W. was funded by a Leverhulme Trust Research Fellowship. G. M. has received funding from the European Unions Horizon 2020 program Blue Action (grant agreement 727852). GRACE is a joint partnership between the National Aeronautics and Space Administration (NASA) in the United States and Deutsche Forschungsanstalt für Luft und Raumfahrt (DLR) in Germany. GRACE ocean data are supported by the NASA MEASUREs Program and are available at <http://grace.jpl.nasa.gov>. Data from the RAPID Climate Change (RAPID)/Meridional Overturning Circulation and Heat flux Array (MOCHA) projects are funded by the Natural Environment Research Council (NERC) and National Science Foundation (NSF, OCE1332978), respectively. Data are freely available from [www.rapid.ac.uk](http://www.rapid.ac.uk) and the British Oceanographic Data Centre ([www.bodc.ac.uk](http://www.bodc.ac.uk)). RAPID is part of the international OceanSITES program ([www.oceansites.org](http://www.oceansites.org)). Florida Current transports are funded by the National Oceanographic and Atmospheric Administration (NOAA) and are available from [www.aoml.noaa.gov/phod/floridacurrent](http://www.aoml.noaa.gov/phod/floridacurrent). Special thanks to the captains, crews, and technicians, who have been invaluable in the measurement of the MOC from moorings in the Atlantic over the past 18 years.

## References

- Baringer, M. O., & Larsen, J. C. (2001). Sixteen years of Florida current transport at 27°N. *Geophysical Research Letters*, 28(16), 3179–3182. <https://doi.org/10.1029/2001GL013246>
- Bendat, J., & Piersol, A. (2010). *Random data: Analysis and measurement procedures* (pp. 79–105). Hoboken, NJ, USA: John Wiley & Sons.
- Bingham, R. J., & Hughes, C. W. (2006). Observing seasonal bottom pressure variability in the North Pacific with GRACE. *Geophysical Research Letters*, 33, L08607. <https://doi.org/10.1029/2005GL025489>
- Böning, C., Timmermann, R., Macrander, A., & Schröter, J. (2008). A pattern-filtering method for the determination of ocean bottom pressure anomalies from GRACE solutions. *Geophysical Research Letters*, 35, L18611. <https://doi.org/10.1029/2008GL034974>
- Bryden, H. L., Mujahid, A., Cunningham, S. A., & Kanzow, T. (2009). Adjustment of the basin-scale circulation at 26°N to variations in Gulf Stream, deep western boundary current and Ekman transports as observed by the Rapid array. *Ocean Science*, 5(4), 421–433. <https://doi.org/10.5194/osd-6-871-2009>
- Bryden, H. L., Saunders, P. M., & Johns, W. E. (2005). Deep western boundary current east of Abaco: Mean structure and transport. *Journal of Marine Research*, 63(1), 35–57.
- Chambers, D. P., & Bonin, J. A. (2012). Evaluation of Release-05 GRACE time-variable gravity coefficients over the ocean. *Ocean Science*, 8(5), 859–868. <https://doi.org/10.5194/os-8-859-2012>
- Cunningham, S. A. (2009). RRS Discovery Cruise D334, 27 Oct–24 Nov 2008. RAPID Mooring Cruise Report.
- DiNezio, P. N., Gramer, L. J., Johns, W. E., Meinen, C. S., & Baringer, M. O. (2009). Observed interannual variability of the Florida Current: Wind forcing and the North Atlantic Oscillation. *Journal of Physical Oceanography*, 39(3), 721–736. <https://doi.org/10.1175/2008JPO4001.1>
- Geruo, A., Wahr, J., & Zhong, S. (2013). Computations of the viscoelastic response of a 3-D compressible Earth to surface loading: An application to glacial isostatic adjustment in Antarctica and Canada. *Geophysical Journal International*, 192(2), 557–572. <https://doi.org/10.1093/gji/ggs030>
- Hughes, C. W., Williams, J., Blaker, A., Coward, A., & Stepanov, V. (2018). A window on the deep ocean: The special value of ocean bottom pressure for monitoring the large-scale, deep-ocean circulation. *Progress in Oceanography*, 161, 19–46. <https://doi.org/10.1016/j.pocean.2018.01.011>
- Intergovernmental Oceanographic Commission (2002). Manual on sea-level measurement and interpretation, Vol. III : Reappraisals and recommendations as of the year 2000. Intergovernmental Oceanographic Commission manuals and guides: 14, Volume III, Paris: Intergovernmental Oceanographic Commission.
- Jackson, L. C., Kahana, R., Graham, T., Ringer, M. A., Woollings, T., Mecking, J. V., & Wood, R. A. (2015). Global and European climate impacts of a slowdown of the AMOC in a high resolution GCM. *Climate Dynamics*, 45(11–12), 3299–3316. <https://doi.org/10.1007/s00382-015-2540-2>
- Johns, W. E., Baringer, M. O., Beal, L. M., Cunningham, S. A., Kanzow, T., Bryden, H. L., et al. (2011). Continuous, array-based estimates of Atlantic ocean heat transport at 26.5°N. *Journal of Climate*, 24(10), 2429–2449. <https://doi.org/10.1175/2010JCLI3997.1>
- Johns, W. E., Kanzow, T., & Zantopp, R. (2005). Estimating ocean transports with dynamic height moorings: An application in the Atlantic Deep Western Boundary Current at 26°N. *Deep Sea Research Part I: Oceanographic Research Papers*, 52(8), 1542–1567. <https://doi.org/10.1016/j.dsr.2005.02.002>
- Kanzow, T., Cunningham, S. A., Rayner, D., Hirschi, J. J.-M., Johns, W. E., Baringer, M. O., et al. (2007). Observed flow compensation associated with the MOC at 26.5°N in the Atlantic. *Science*, 317(5840), 938–941. <https://doi.org/10.1126/science.1141293>
- Kanzow, T., Flechtner, F., Chave, A., Schmidt, R., Schwintzer, P., & Send, U. (2005). Seasonal variation of ocean bottom pressure derived from Gravity Recovery and Climate Experiment (GRACE): Local validation and global patterns. *Journal of Geophysical Research*, 110, C09001. <https://doi.org/10.1029/2004JC002772>
- Kanzow, T., Johnson, H. L., Marshall, D. P., Cunningham, S. A., Hirschi, J. J.-M., Mujahid, A., et al. (2009). Basinwide integrated volume transports in an eddy-filled ocean. *Journal of Physical Oceanography*, 39(12), 3091–3110. <https://doi.org/10.1175/2009JPO4185.1>
- Landerer, F. W., Wiese, D. N., Bentel, K., Boening, C., & Watkins, M. M. (2015). North Atlantic meridional overturning circulation variations from GRACE ocean bottom pressure anomalies. *Geophysical Research Letters*, 42, 8114–8121. <https://doi.org/10.1002/2015GL065730>
- Lee, T. N., Johns, W. E., Zantopp, R. J., & Fillenbaum, E. R. (1996). Moored observations of western boundary current variability and thermohaline circulation at 26.5°N in the subtropical North Atlantic. *Journal of Physical Oceanography*, 26(6), 962–983.
- Macrander, A., Böning, C., Boebel, O., & Schröter, J. (2010). Validation of GRACE gravity fields by in-situ data of ocean bottom pressure. In F. M. Flechtner, et al. (Eds.), *System Earth via geodetic-geophysical space techniques* (pp. 169–185). Berlin, Heidelberg: Springer Berlin Heidelberg.
- McCarthy, G., Frajka-Williams, E., Johns, W. E., Baringer, M. O., Meinen, C. S., Bryden, H. L., et al. (2012). Observed interannual variability of the Atlantic meridional overturning circulation at 26.5°N. *Geophysical Research Letters*, 39, L19609. <https://doi.org/10.1029/2012GL052933>
- McCarthy, G. D., Smeed, D. A., Johns, W. E., Frajka-Williams, E., Moat, B. I., Rayner, D., et al. (2015). Measuring the Atlantic Meridional Overturning Circulation at 26°N. *Progress in Oceanography*, 130, 91–111. <https://doi.org/10.1016/j.pocean.2014.10.006>
- McDougall, T. J., & Barker, P. M. (2011). Getting started with TEOS 10 and the Gibbs Seawater (GSW) Oceanographic Toolbox. SCOR/IAPSO WG127.
- Meinen, C. S., Baringer, M. O., & Garcia, R. F. (2010). Florida Current transport variability: An analysis of annual and longer-period signals. *Deep-Sea Research Part I*, 57, 835–846.
- Meinen, C. S., Johns, W. E., Garzoli, S. L., van Sebille, E., Rayner, D., Kanzow, T., & Baringer, M. O. (2013). Variability of the deep western boundary current at 26.5°N during 2004–2009. *Deep Sea Research Part II: Topical Studies in Oceanography*, 85, 154–168. <https://doi.org/10.1016/j.dsr2.2012.07.036>

- Park, J., Watts, D. R., Donohue, K. A., & Jayne, S. R. (2008). A comparison of in situ bottom pressure array measurements with GRACE estimates in the Kuroshio Extension. *Geophysical Research Letters*, 35, L17601. <https://doi.org/10.1029/2008GL034778>
- Percival, D. B., & Walden, A. T. (1998). *Spectral analysis for physical applications : Multitaper and conventional univariate techniques*. Cambridge, New York: Cambridge University Press.
- Rhines, P. B., Hakkinen, S., & Josey, S. A. (2008). *Is oceanic heat transport significant in the climate system?* Berlin, Germany: Springer Verlag.
- Smeed, D. A., Josey, S. A., Beaulieu, C., Johns, W. E., Moat, B. I., Frajka-Williams, E., et al. (2018). The North Atlantic Ocean is in a state of reduced overturning. *Geophysical Research Letters*, 45, 1527–1533. <https://doi.org/10.1002/2017GL076350>
- Smeed, D. A., McCarthy, G. D., Cunningham, S. A., Frajka-Williams, E., Rayner, D., Johns, W. E., et al. (2014). Observed decline of the Atlantic meridional overturning circulation 2004–2012. *Ocean Science*, 10(1), 29–38. <https://doi.org/10.5194/os-10-29-2014>
- Smeed, D., McCarthy, G., Rayner, D., Moat, B., Johns, W., Baringer, M., & Meinen, C. (2015). Atlantic meridional overturning circulation observed by the RAPID-MOCHA-WBTS (RAPID-Meridional Overturning Circulation and Heatflux Array-Western Boundary Time Series) array at 26°N from 2004 to 2017. <https://doi.org/10.5285/1a774e53-7383-2e9a-e053-6c86abc0d8c7>
- Stocker, T. F., Qin, D., Plattner, G.-K., Tignor, M., Allen, S., Boschung, J., Nauels, A., Xia, Y., Bex, V., & Midgley, P. (Eds.) (2013). *Climate change 2013 : The physical science basis : Working Group I Contribution to the Fifth Assessment Report of the Intergovernmental Panel on Climate Change* (pp. 1535). Cambridge, New York: Cambridge University Press, 2014
- Thomson, R. E., & Emery, W. J. (2014). Data analysis methods in physical oceanography. In R. E. Thomson, & W. J. Emery (Eds.), *Chapter 5—Time series analysis methods* (pp. 425–591). Boston: Elsevier. <https://doi.org/10.1016/B978-0-12-387782-6.00005-3>
- Wahr, J., Nerem, R. S., & Bettadpur, S. V. (2015). The pole tide and its effect on GRACE time-variable gravity measurements: Implications for estimates of surface mass variations. *Journal of Geophysical Research: Solid Earth*, 120, 4597–4615. <https://doi.org/10.1002/2015JB011986>
- Watkins, M. M., Wiese, D. N., Yuan, D., Boening, C., & Landerer, F. W. (2015). Improved methods for observing Earth's time variable mass distribution with GRACE using spherical cap mascons. *Journal of Geophysical Research: Solid Earth*, 120, 2648–2671. <https://doi.org/10.1002/2014JB011547>
- Watts, D. R., & Kontoyiannis, H. (1990). Deep-ocean bottom pressure measurement—Drift removal and performance. *Journal of Atmospheric & Oceanic Technology*, 7(2), 296–306.
- Wiese, D. N., Landerer, F. W., & Watkins, M. M. (2016). Quantifying and reducing leakage errors in the JPL RL05M GRACE mascon solution. *Water Resources Research*, 52, 7490–7502. <https://doi.org/10.1002/2016WR019344>
- Wiese, D. N., Yuan, D.-N., Boening, C., Landerer, F. W., & Watkins, M. M. (2015). JPL GRACE Mascon Ocean, ice, and hydrology equivalent water height JPL RL05M.1. Ver. 1. PO.DAAC, CA, USA. Dataset accessed [2017-01-30] at <https://doi.org/10.5067/TEMSC-OCL05>